

# Organotrifluoroborate Sugar Conjugates for a Guided Boron Neutron Capture Therapy: From Synthesis to Positron Emission Tomography

Laura Confalonieri, Daniela Imperio,\* Alvaro Erhard, Silvia Fallarini, Federica Compostella, Erika del Grosso, Marcin Balcerzyk,\* and Luigi Panza



Cite This: *ACS Omega* 2022, 7, 48340–48348



Read Online

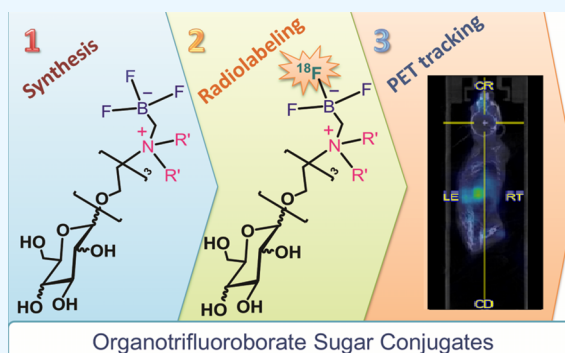
ACCESS |

Metrics & More

Article Recommendations

Supporting Information

**ABSTRACT:** Sugars are a versatile tool for targeting malignant cells and have been extensively used for drug delivery and imaging techniques. Their prototype, fluorodeoxyglucose ( $[^{18}\text{F}]\text{FDG}$ ), is currently used for positron emission tomography. Boron neutron capture therapy (BNCT) is a cancer treatment that relies on irradiation with thermal neutrons of cancer cells previously loaded with  $[^{10}\text{B}]$ -containing compounds. The recent introduction of accelerators as a neutron source for clinical use prompts the planning of delivery compounds enriched with boron able to be traced in real time. This work describes the first synthesis of a new class of sugar derivatives conjugated to a trifluoroborate moiety as potential theranostic agents. Stability and cytotoxicity studies are reported for all compounds, together with  $[^{18}\text{F}]$  radiolabeling optimization and *in vivo* preliminary positron emission tomography (PET) experiments on a selected compound.



## 1. INTRODUCTION

BNCT is a binary approach to cancer treatment based on the concomitant administration of boron-containing molecules and irradiation with low-energy neutrons.<sup>1</sup> The capture of a neutron by  $[^{10}\text{B}]$  atoms triggers a fission reaction that destroys the malignant cells. To ensure the best therapeutic results, cancer irradiation should be performed when the concentration of the BNCT agent within the tumor is the highest possible, above 2 mM.<sup>2,3</sup> To date, three boron-containing molecules have been approved for clinical trials and one for clinical use in Japan (boronophenylalanine BPA–Steboronine, Stella Pharma Corporation, Chuo-ku, Osaka, Japan),<sup>4</sup> but all of them are far from ideal, especially because they cannot be traced *in vivo*.<sup>5</sup> As targeted therapy represents a major focus of biomedical research today, to guarantee further development for the BNCT approach, new boron-containing compounds should act as theranostic agents, both delivering the boron atom needed for the therapy and tracking the biodistribution of the molecule in real time.<sup>6,7</sup>

Boronated carbohydrate derivatives have received consideration in BNCT due to the preferential uptake of sugars by tumor cells, prompting us to design new BNCT theranostic agents based on monosaccharide scaffolds.<sup>8–10</sup> Recently, new boronic acid derivatives have been synthesized introducing a boronic acid moiety into the sugar skeleton.<sup>11–14</sup> Of interest is the fact that it has been reported that glucose membrane

transporters tolerate modifications at the anomeric position of the sugar.<sup>15</sup>

Organotrifluoroborates ( $\text{R}-\text{BF}_3^-$ ) represent a very interesting alternative to boronic acids, boronate esters, and organoboranes. They are well known to be crystalline compounds, easy to handle, and quite stable to moisture and air.<sup>16</sup> Vedejs and co-workers first described the facile synthesis of organotrifluoroborates from boronic acids using  $\text{KHF}_2$  as a convenient and inexpensive reagent.<sup>17</sup> Trifluoroborates are also easily accessible from boronate esters, boroxines, or diaminoboranes.<sup>18</sup> Among them, organoboronic acid pinacol esters are stable and versatile precursors of  $\text{R}-\text{BF}_3\text{K}$  salts.

Trifluoroborate salts are usually subjected to fast hydrolysis in both acidic and basic aqueous solutions. A high rate of B–F bond solvolysis is of fundamental importance in cross-coupling reactions but is detrimental to the design of kinetically stable  $[^{18}\text{F}]$  organotrifluoroborates for positron emission tomography (PET) imaging.<sup>19–21</sup> Over the years, several groups have studied the kinetic stability of organotrifluoroborate reagents in

**Received:** October 11, 2022

**Accepted:** November 29, 2022

**Published:** December 12, 2022



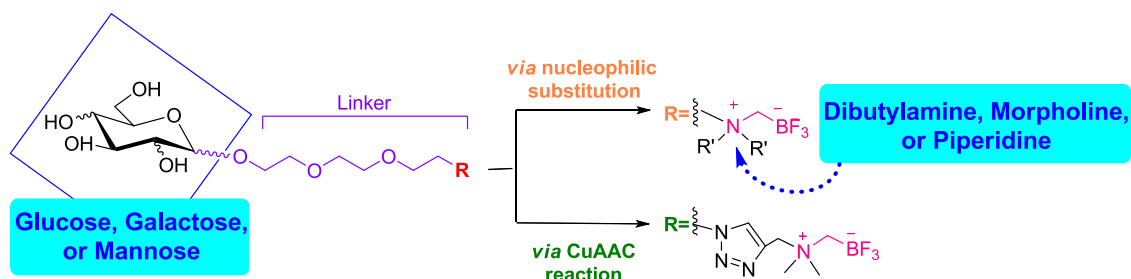


Figure 1. General structure of sugar conjugates.

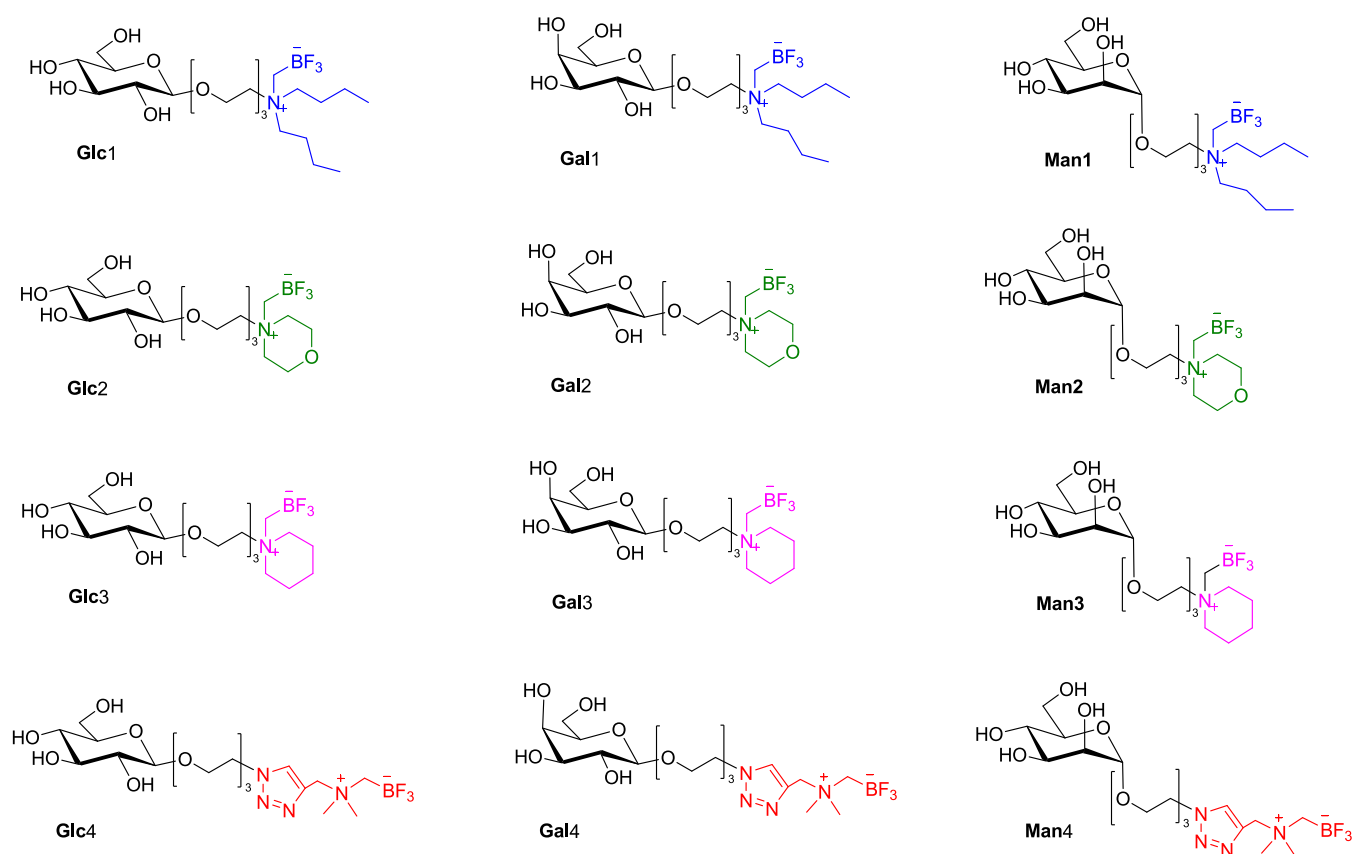


Figure 2. Library of 12 sugar derivative conjugates to a trifluoroborate moiety.

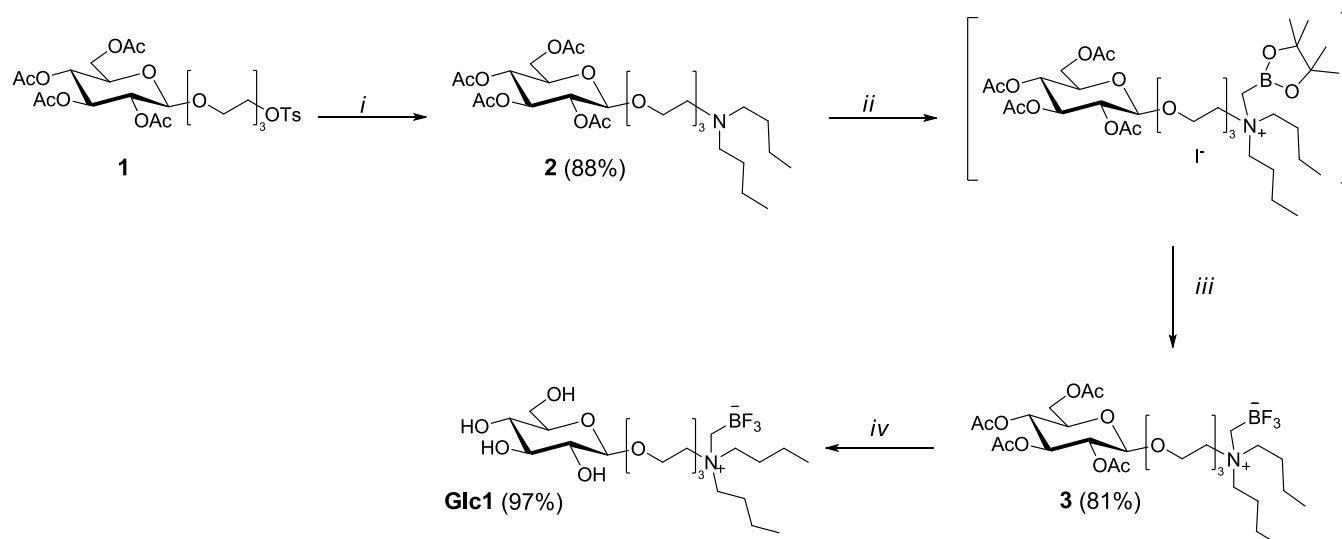
organic solvents and water. As expected, structural changes can dramatically affect the organotrifluoroborate stability. Electron-withdrawing substituents retard the rate of aryltrifluoroborate solvolysis, while electron-donating groups enhance it. In particular, a positive-charged heteroatom in the  $\beta$  position can increase the kinetic stability of nonaromatic organotrifluoroborate in water by several orders of magnitude. In a recent paper, Perrin et al. studied the rate constants of solvolysis at pH 7.5 (phosphate buffer) to mimic physiological blood conditions. They demonstrated that aliphatic trifluoroborates are prone to solvolysis in a few minutes, while when a quaternary onium salt is introduced in the  $\beta$  position, the compounds show stability in solution for days or even months.<sup>22</sup> Therefore, the introduction of this zwitterionic substructure into molecules able to target malignant cells could provide a promising theranostic BNCT agent in which trifluoroborate acts as a carrier of both [<sup>10</sup>B] and [<sup>18</sup>F]. In the literature, a metabolically stable [<sup>18</sup>F]-labeled tyrosine derivative containing a trifluoroborate has been recently

reported.<sup>23</sup> It has to be noted that the exchange of a naturally occurring [<sup>19</sup>F] with [<sup>18</sup>F]—required for PET radiolabeling—does not affect the structure of the molecule, so the tracer has the same chemical and pharmacological properties of the unlabeled molecule potentially useful as a BNCT agent.

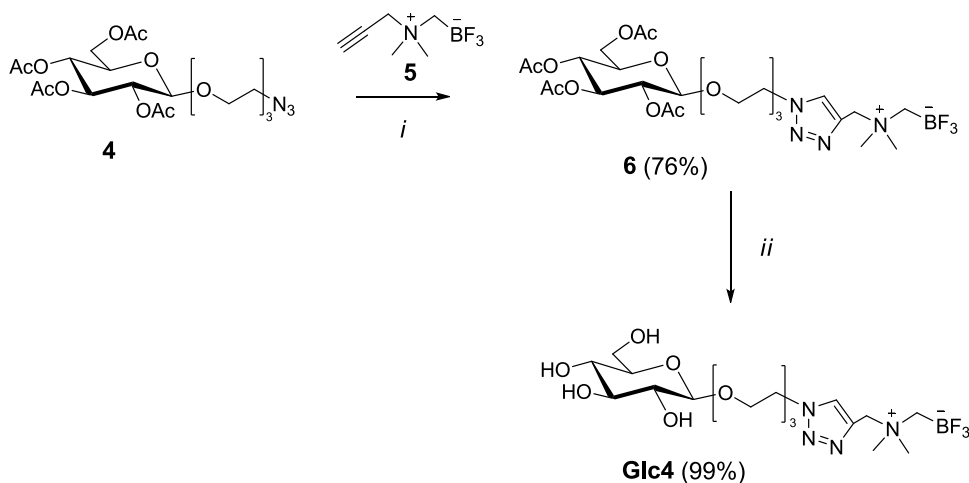
This work reports the synthesis of a library of 12 compounds having the generic structure: monosaccharide—linker—ammonium trifluoroborate group (Figure 1). Their structure differs for the type of monosaccharide—glucose, galactose, or mannose—and for the alkyl residue of the ammonium portion, varied to modulate the hydrophobicity and steric hindrance around the zwitterionic portion of the trifluoroborate. The synthesis of the target compounds is based on two different synthetic strategies starting from a common intermediate, one relying on a nucleophilic substitution and the other involving a click reaction.

The toxicity of the target compounds is assessed on human fibroblasts, followed by evaluation of the stability of the trifluoroborate group at physiological pH by NMR analysis of

**Scheme 1. Synthesis of Glc1:** (i) Dibutylamine, CH<sub>3</sub>CN, 82 °C; (ii) Iodomethylboronyl Pinacolate, Et<sub>2</sub>O, rt; (iii) KHF<sub>2</sub>, CH<sub>3</sub>CN, H<sub>2</sub>O, rt; and (iv) KOH, MeOH, rt



**Scheme 2. Synthesis of Glc4:** (i) Sodium Ascorbate, CuSO<sub>4</sub>·5H<sub>2</sub>O, *t*-BuOH, H<sub>2</sub>O, rt and (ii) KOH, MeOH, rt



the four glucose-containing compounds **Glc1–4** (see [Figure 2](#)). It has been assumed that all of the compounds with the same zwitterionic part share the same stability since the sugar part, being far from the BF<sub>3</sub> group, should exert a negligible influence on BF<sub>3</sub> stability. Then, two glucose-containing compounds, namely, **Glc1** and **Glc4**, are selected because of the relevance of glucose in tumor metabolism. As our main interest is the theranostic aspect, we decided to directly move to PET imaging. Therefore, the [<sup>18</sup>F] labeling protocol for the PET experiments is studied and optimized. One of the two candidates is finally used for preliminary PET analysis on mice.

## 2. RESULTS AND DISCUSSION

**2.1. Chemistry.** [Figure 2](#) shows the structures of the library of sugar conjugates described in this work.

Before starting, it was necessary to carefully plan the synthesis to define the proper synthetic sequence and to identify the better protecting groups for the sugar part because not much is known about the stability of zwitterionic trifluoroborates.

Acetates were selected as sugar protecting groups since they allow easy control over the glycosylation stereochemistry

outcome. Also, they can be removed in mild acidic or basic conditions even if it is not possible to exclude *a priori* the possibility of a concomitant alcoholysis of the BF<sub>3</sub> group. The other most popular hydroxyl protecting groups for sugars, namely, benzyl ethers, were discarded both because their installation would have required more steps to ensure the formation of a single anomer and, predominantly, for concerns about the compatibility of trifluoroborate with the catalytic hydrogenation required for their removal.

A biocompatible triethylene glycol spacer was introduced in all structures to outdistance the sugar structure from the trifluoroborate moiety. In general, PEG is a widely used polymer in various formulations due to its biocompatibility. PEGylation of proteins, drugs, and bioactive molecules is known to increase the solubility of hydrophobic compounds in aqueous medium, extend the circulation time, reduce the nonspecific uptake, and achieve specific tumor targetability.<sup>24</sup>

The overall synthetic pathway was first tested and optimized on glucose ([Scheme 1](#)). Treatment of the known monotosylated glucosyl derivative **1**<sup>25</sup> with an excess of dibutylamine in acetonitrile at reflux gave the corresponding tertiary amine **2** in satisfactory yield. The nitrogen atom was then alkylated with

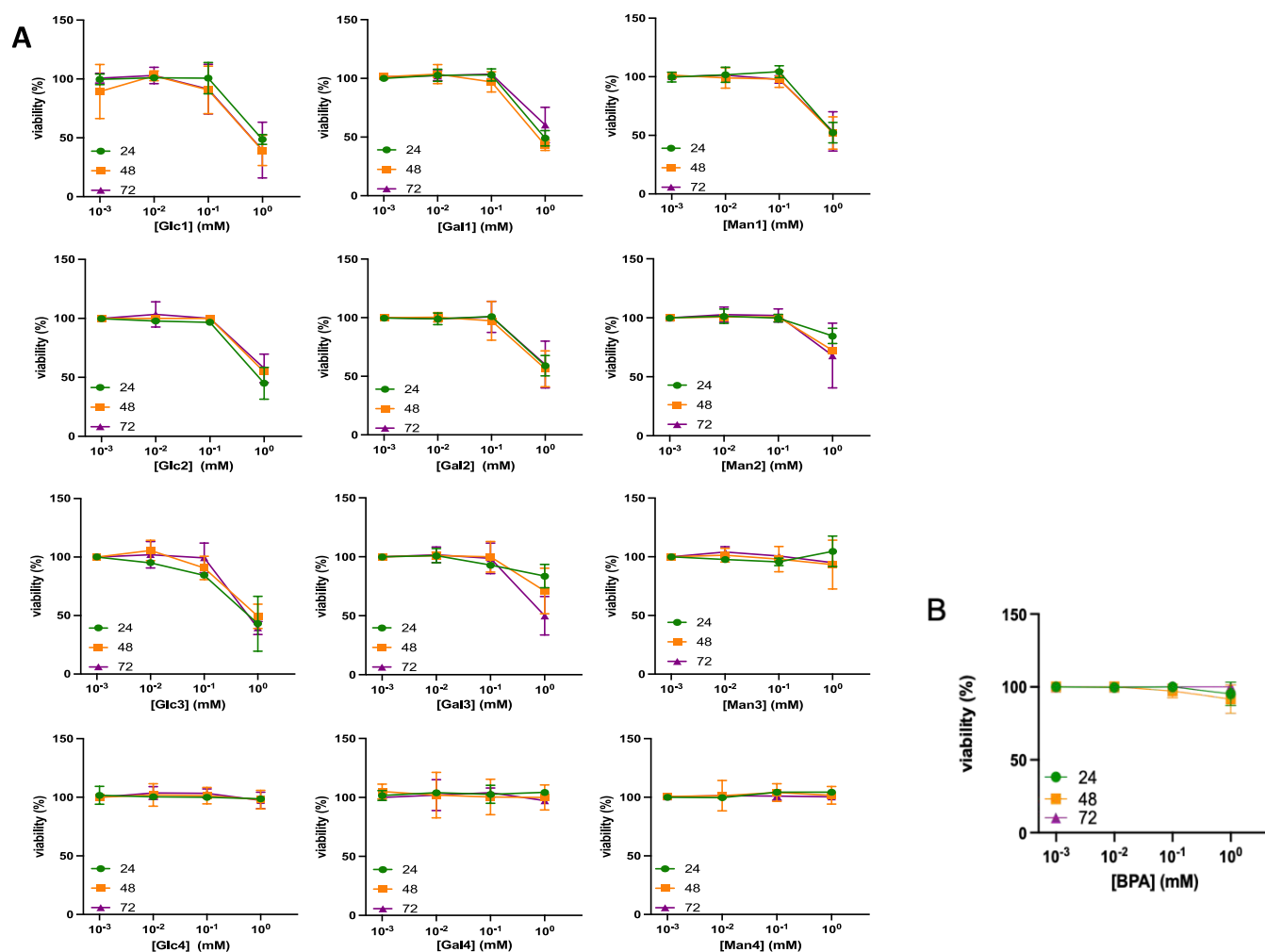


**Figure 3.** Effects of (A) tested compounds (Glc1–4, Gal1–4, and Man1–4) and (B) boronophenylalanine (BPA) on cell viability. The effects of tested compounds on human primary fibroblast viability were assessed by an MTT assay after 24, 48, and 72 h of treatment with increasing concentrations (0.001–1 mM) of each compound. The concentration–response curves show the percentage of cells. The data represent the mean  $\pm$  SD of at least three independent experiments run in triplicate.

iodomethylboronyl pinacolate in diethyl ether at room temperature. In a first attempt to obtain the desired final compound, deacetylation was attempted on the intermediate quaternary ammonium salt, but the purification of the deprotected product was very difficult. So, the boronyl pinacolate was converted into the trifluoroborate by treatment of the crude quaternary salt with an aqueous solution of potassium hydrogen fluoride. In this way, compound **3** was obtained in satisfactory yield after purification on silica gel.

Finally, the last deprotection step, performed with a catalytic amount of base in methanol, allowed us to obtain the first target product **Glc1**. The conditions employed for removing the acetate esters did not affect the trifluoroborate group.

The same optimized scheme was used for the synthesis of the other target compounds. **Glc2** and **Glc3** were obtained in comparable yields by changing the secondary amine in the first reaction on compound **1**. Then, the synthesis was repeated by changing the sugar moiety and the corresponding galactose and mannose derivatives **Gal1**, **Gal2**, **Gal3**, **Man1**, **Man2**, and **Man3** were obtained smoothly (see the Supporting Information for the experimental details).

To shorten the synthetic scheme, a second series of derivatives were obtained by exploiting a copper-catalyzed

azide–alkyne cycloaddition (CuAAC, click reaction) (Scheme 2). The azido compound **4**<sup>26</sup> was obtained according to the literature from the tosyl derivative **1**. The reaction of compound **4** with the known zwitterionic alkynyl trifluoroborate **5**<sup>22</sup> in the presence of aqueous copper sulfate and sodium ascorbate smoothly afforded the expected cycloaddition triazole derivative **6** with a satisfactory yield.

The deprotection of compound **6** with a catalytic amount of potassium hydroxide in methanol provided the target molecule **Glc4**.

The final compound **Glc4** did not require any further purification (purity >95% by NMR). The same strategy was exploited for the preparation of D-galactose and D-mannose triazole derivatives named **Gal4** and **Man4** (see Supporting Information Scheme S4 for details).

**2.2. Cytotoxicity.** To evaluate the effect of tested compounds and BPA on cell viability, human primary fibroblasts were used (Figure 3). BPA was chosen as the reference compound as it is the compound most frequently used in clinical studies of BNCT and is a drug approved for clinical use in Japan. Cells were treated (24–72 h) with increasing concentrations (0.001–1 mM) of each compound, and cell viability was measured by an MTT assay. No toxicity



was measured up to 100  $\mu\text{M}$ , but at 1 mM, differences in cell viability started to be observed. Like BPA, the library of triazole conjugates (**Glc4**, **Gal4**, and **Man4**) and **Man3** did not show toxicity also at 1 mM. Differently, the other compounds (**Glc1–3**, **Gal1–3**, and **Man1–2**) at 1 mM induced a reduction of cell viability at all times considered when compared with BPA. As a general trend, the compounds of the first series demonstrate to be toxic at the higher concentration tested, while triazole-containing derivatives have negligible toxicity.

**2.3.  $^{19}\text{F}$  NMR Stability Studies.** The stability of the trifluoroborate groups was analyzed in pseudophysiological conditions through  $^{19}\text{F}$  NMR spectroscopy. According to the literature, this technique is sensitive enough to detect  $^{19}\text{F}$ -chemical shifts that correspond to the starting trifluoroborate, any intermediate products, and free fluoride.<sup>22,27</sup> The experiment was performed on glucose derivatives **Glc1–4**, to assess if the stability of the trifluoroborate group could be affected by structural changes in an ammonium moiety. Each compound was dissolved in phosphate buffer (pH 7.5) at a very low concentration (2 mg/mL) to assure a pseudo-first-order kinetic. The  $^{19}\text{F}$  spectra were acquired at fixed times (320 scans, 298 K). The peaks of the starting material (ca.  $-135$  ppm) and of the free fluoride (ca.  $-120$  ppm) were integrated and plotted in the graph showing the fraction of the starting material present ( $[\text{BF}_3]/([\text{BF}_3] + [\text{F}^-])$ ) versus time values ( $t$ ) (see the Supporting Information for details). The results were fit to the equation  $([\text{BF}_3]/([\text{BF}_3] + [\text{F}^-]))_t = ([\text{BF}_3]/([\text{BF}_3] + [\text{F}^-]))_0 \times e^{-kt}$  to calculate the rate constants ( $k$ ) and half-life value ( $t_{1/2}$ ) for each tested compound. **Glc3** was found to be the less stable compound with a  $k$  of  $4 \times 10^{-2}$  and a half-life value of 24 h. **Glc4** was the more stable compound with a  $k$  which is 2 orders of magnitude smaller ( $7 \times 10^{-4}$ ) than that of **Glc3** and an extrapolated half-life value of 40 days. **Glc1** and **Glc2** showed comparable hydrolysis behaviors with half-life values of 72 and 120 h, respectively.

The greater stability of **Glc4** can be a possible explanation for its lower toxicity and for the difficulties experienced in the labeling procedure optimization as reported in paragraph 2.5.

**2.4. HR-MS Stability Studies on **Glc1** and **Glc4** for the Optimization of Labeling Conditions.** The stability of compounds **Glc1** and **Glc4** were first studied at different temperatures and pH with thin-layer chromatography (TLC) to assess the best conditions for the labeling procedure. Solutions of **Glc1** and **Glc4** were prepared separately (1 mg each in 0.5 mL of demineralized water), and the pH was adjusted to 0.5 and 2 for each compound. A similar behavior was observed for both compounds. The mixtures were warmed at 85  $^\circ\text{C}$ , and TLCs were run after 15 min. At pH 0.5, an extensive degradation was observed, while at pH 2, the compound degraded only partially. At this point, the procedure was repeated at 40  $^\circ\text{C}$  only at pH 2. TLCs were run after 15, 30, and 60 min. No byproducts were detected (data not shown). In addition, to characterize the nature of the degraded products obtained at acidic pH, mass spectrometry experiments were performed for **Glc1**. **Glc1** was dissolved in 100  $\mu\text{L}$  of a solution of KF ( $3.7 \times 10^{-9}$  M), and the pH was adjusted to 2 with HCl 1 N. The mixture was warmed at 85  $^\circ\text{C}$ , and mass spectrometry analyses were performed at rt at time zero ( $t_0$ ) and after 15 min ( $t_1$ ), 30 min ( $t_2$ ), 45 min ( $t_3$ ), and 60 min ( $t_4$ ). The main byproduct observed, as expected, was the boronic acid derivative whose concentration tends to increase in the function of time. Considering the issue of the half-time

of  $^{18}\text{F}$  in the labeled form of the target compounds, we decided to study a purification step from boronic acid derivative through an alumina cartridge (Sep-Pak) after 20 min at 85  $^\circ\text{C}$ ; in these conditions, the HR-MS analyses confirmed the presence of almost only **Glc1** (see the Supporting Information).

**2.5. Radiolabeling Procedure on **Glc4** and **Glc1** and Stability Studies.** The radiolabeling approach was planned at first according to literature procedures. Several authors suggest radioisotopic exchange reactions using  $^{18}\text{F}$  as a rapid, simple, and efficient manner for direct radiolabeling of trifluoroborate groups in biomolecules using room temperature.<sup>28–30</sup>

Typically, the exchange is accomplished by treatment of the trifluoroborate with  $^{18}\text{F}$  fluoride in acidic conditions at different concentrations and temperatures. A series of experiments were performed by modifying these parameters and evaluating the purity and the radiochemical yield.

In an initial experiment, before the HR-MS studies, the reaction was tried on 500 nmol of both compounds by treatment of the solid **Glc1** or **Glc4** with a solution of  $^{18}\text{F}$  fluoride directly obtained from the cyclotron (1.85–2.22 GBq in 50 mL of unfixed target  $^{18}\text{O}$  water) and the pH adjusted to 2.0 by addition of a small amount of 0.5 M HCl. The solutions were warmed at 40 or 85  $^\circ\text{C}$ , and the radiolabeling kinetics were monitored by radio-TLC at different times (10, 15, 20, 30, 60, 90, 120, and 150 min at 40  $^\circ\text{C}$  or 10, 15, and 20 or 15, 30, and 60 min at 85  $^\circ\text{C}$ ) using radio-TLC equipment. (see the Supporting Information for all experimental details).

**Glc4** did not show any radiolabeling at any time and temperature; therefore, the radiolabeling was optimized on **Glc1**. The protocol was repeated on **Glc1** at 40  $^\circ\text{C}$ , obtaining a conversion of about 63% at 120 min and a radiolabeled purity of 96.9% after purification.

When **Glc1** was radiolabeled in the same conditions but at 85  $^\circ\text{C}$ , a conversion of 42% at 20 min and a final radiolabeled purity of 96.6% were achieved. As expected, the higher temperature allowed high radiolabeling in a shorter time.

The suitability of radiolabeling using a semiautomated radiochemical synthesis module was then evaluated. In this case, **Glc1** was previously dissolved in a physiological solution and treated with a  $^{18}\text{F}$  solution obtained by trapping  $^{18}\text{F}$  in a QMA cartridge and then eluting with a physiological solution. The reaction at 40  $^\circ\text{C}$  gave a conversion of 23.1% at 120 min, while at 85  $^\circ\text{C}$  the conversion was 41.7% at 60 min. The promising results prompted us to reproduce the procedure in an automated synthesis module (TracerLAB FX-FN). It was necessary to purify the final compound twice to obtain a purity of 98% but with a very low radiochemical yield, probably for the very diluted conditions. The automated procedure was then abandoned, and the following improved procedure was tested.

First, fluoride solution was obtained by trapping  $^{18}\text{F}$  in a PS- $\text{HCO}_3$  Chromafix small cartridge. Then, the solution was eluted with a physiological solution acidified with 0.5 M HCl to obtain an acidified  $^{18}\text{F}$  solution. This procedure not only allows us to eliminate Havar window contaminants from the cyclotron but also avoids any irradiation of the operator.

**Glc1** was then dissolved in the acidic  $^{18}\text{F}$  solution and warmed at 85  $^\circ\text{C}$ . After 20 min, the conversion was 49.88%, and by purification on a Sep-Pak alumina cartridge, labeled **Glc1** was obtained with a radiolabeled purity of 97.2% (see the Supporting Information, Figure S7). The reproducibility was confirmed by six times of repetition of the radiolabeling. The

**Table 1. Results of the Different Radiolabeling Methods Applied to Glc1<sup>a</sup>**

[ <sup>18</sup> F] source	precursor	temperature (°C)	maximum RCY (%)	time max RCY (min)	purity after alumina (%)
direct from cyclo	solid	40	63.4	120	96.9
direct from cyclo	solid	85	42.4	20	96.6
direct from cyclo	dissolved	40	23.1	150	<sup>b</sup>
direct from cyclo	dissolved	85	41.7	60	<sup>b</sup>
acidified [ <sup>18</sup> F]	solid	85	49.88	20	97.2

<sup>a</sup>The method described as “direct from cyclo” means that [<sup>18</sup>F]fluorine was used without any purification and obtained from the liquid [<sup>18</sup>O] target. We only represent the maximum radiochemical yield (RCY) obtained by radio-TLC and the time where this RCY was obtained with the purity of the compound [<sup>18</sup>F]Glc1 when purification was made with an alumina cartridge. <sup>b</sup>No purification was made when a manual procedure using a dissolved precursor was used.

results obtained in the different conditions tested are summarized in Table 1.

To investigate the applicability of [<sup>18</sup>F]Glc1 radiolabeled compound, the *in vitro* stability in physiological solution and in human plasma was investigated. The stability limit was assumed as the time when the radiolabeled compound purity decreases to 95%, which involves an amount of free [<sup>18</sup>F]fluorine of 5%, which could negatively interfere with the quality of the microPET images. At 37 °C, we found that [<sup>18</sup>F]Glc1 was stable for 1 h in human plasma and for 100 min in physiological solution (Figure 4).

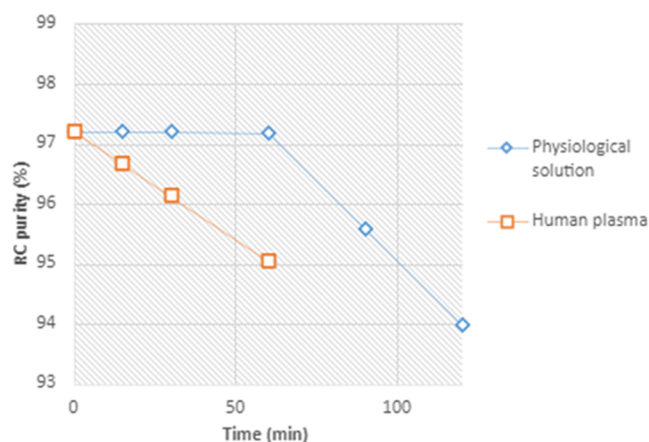


**Figure 4.** Radiolabeling stability for [<sup>18</sup>F]Glc1 when an acidified [<sup>18</sup>F] method was used at 85 °C, studied in physiological solution and human plasma. The stability of [<sup>18</sup>F]Glc1 in human plasma was 60 min and stability in physiological solution was 100 min.

**2.6. MicroPET Verification of [<sup>18</sup>F]Glc1 Compared to [<sup>18</sup>F]FDG.** As the introduction of [<sup>18</sup>F] in the molecule allows us to follow directly the biodistribution *in vivo* of Glc1, we decided to avoid the preliminary test of cellular uptake and directly perform a PET experiment. We were aware that this experiment can only give indication on quantitative uptake, which is important for potential BNCT application, but we presumed that the biodistribution *in vivo* of Glc1 in comparison with the behavior of FDG could have given at least preliminary suggestions on the involvement of glucose transporters.

The results of the PET/CT scan with [<sup>18</sup>F]Glc1 are shown in Figure 5A and can be compared to the [<sup>18</sup>F]FDG scan shown in Figure 5B. The preliminary result of the incorporation of the drug Glc1 from its PET/CT scan in healthy mice indicates that the drug is metabolized in the liver, does not pass the blood–brain barrier, and is not metabolized in the heart (Figure 5A). The detailed comparison of the

uptake in the brain is shown in Figure 5C. The [<sup>18</sup>F]Glc1 uptake in the center of the brain is about 0.08 standard uptake value (SUV), while that of [<sup>18</sup>F]FDG is about 1.6 SUV, about 20 times more. The detailed comparison of the uptake in the heart is shown in Figure 5D. The [<sup>18</sup>F]Glc1 uptake in the center of the heart is about 0.2 SUV, while that of [<sup>18</sup>F]FDG is about 2.7 SUV, about 14 times more. There is also no uptake of [<sup>18</sup>F]Glc1 in the bones, which show that no free [<sup>18</sup>F] disconnected from the drug is circulating in the blood, confirming the compound stability within the time of PET experiment. In the control experiment, the metabolism of [<sup>18</sup>F]FDG shows typical metabolism in the heart, brain, and brown fat (Figure 5B). We assumed that the radio-pharmaceutical derivative of glucose for BNCT will follow the metabolic pathway of glucose and therefore FDG. This is not the case for [<sup>18</sup>F]Glc1.

### 3. CONCLUSIONS

In this paper, we described the preparation of a small library of 12 sugars conjugated through triethylene glycol to a trifluoroborate moiety. The developed synthesis proved to be robust and efficient, and the final compounds demonstrated to be stable in the final deprotection step and easily purifiable. The derivatives Glc1–3, Gal1–3, and Man1–3 showed toxicity on human fibroblasts only at very high concentrations, which makes them suitable for PET but not for BNCT. On the other hand, the derivatives Glc4, Gal4, and Man4 having a triazole moiety showed low toxicity also at the highest concentrations tested. The radiolabeling of Glc1 required some optimization and gave sufficiently pure [<sup>18</sup>F]Glc1. As evaluated by PET images, [<sup>18</sup>F]Glc1 in mice accumulated mainly in the liver and kidneys, telling us that these compounds follow a different biodistribution and metabolism with respect to FDG, therefore suggesting that its biodistribution does not involve glucose transport proteins. In conclusion, this study demonstrates that the synthesis of sugar derivatives containing the –BF<sub>3</sub> moiety is feasible in a simple, efficient, and rapid manner. Radiolabeling with [<sup>18</sup>F] was successfully achieved on one derivative, and the radiotracer was demonstrated to be enough stable both *in vitro* and *in vivo* when injected into mice for imaging with microPET. On the other hand, the same compound appears to be quite toxic for BNCT applications. The discovery of a potential theranostic candidate for BNCT remains a big challenge for researchers. Taking into account these preliminary and encouraging results, having in hand a consolidated synthetic procedure and a protocol for radiolabeling work in progress for the extension to other sugars containing trifluoroborates *en route* toward new potential theranostic derivatives, able to target malignant cells.

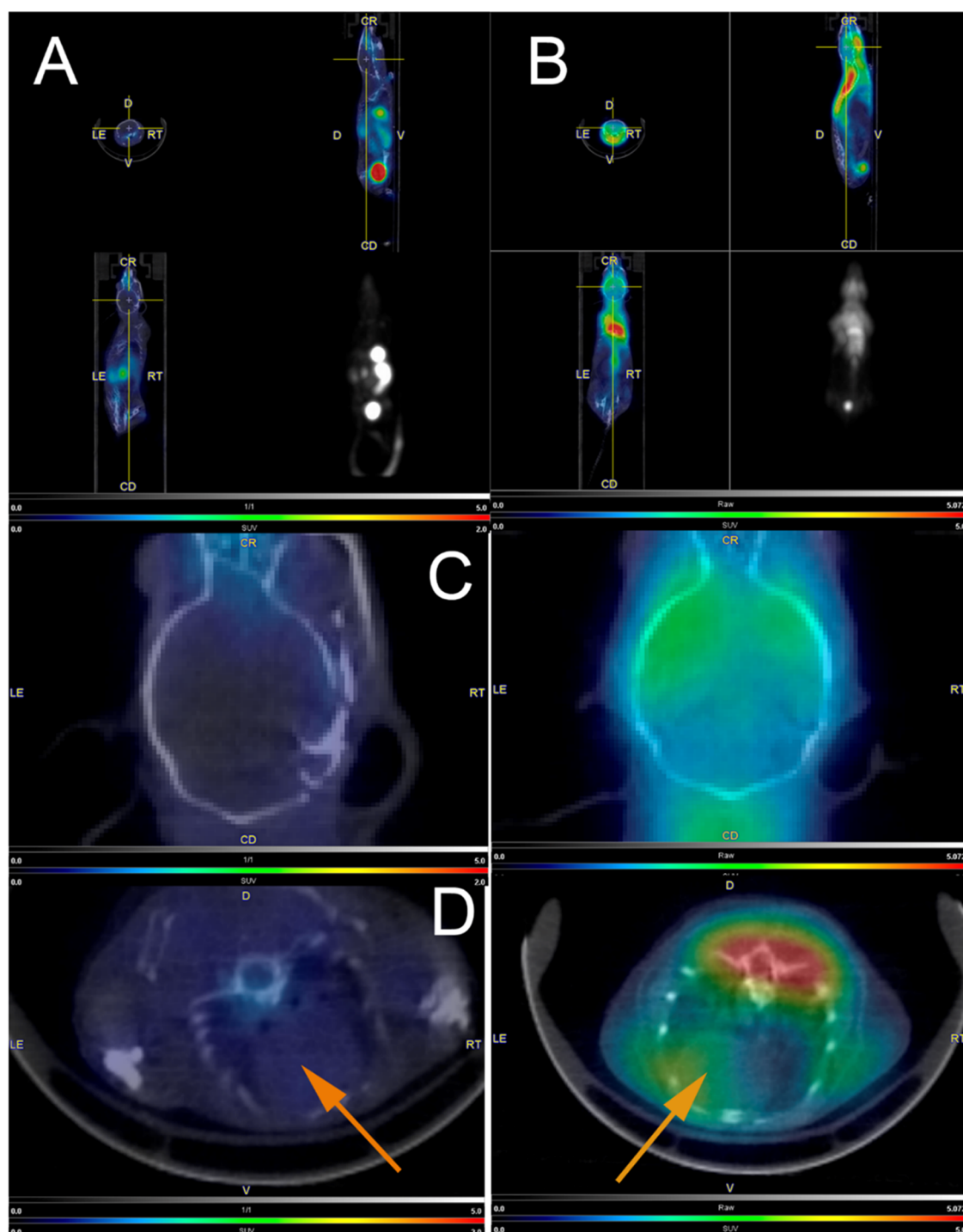


**Figure 5.** (A) PET/CT study of the radiopharmaceutical [ $^{18}\text{F}$ ]Glc1 in healthy mice. Uptake in the liver and elimination through the bladder are observed. No metabolism is observed in the brain or heart. (B) PET/CT study of the radiopharmaceutical [ $^{18}\text{F}$ ]FDG in healthy mouse. The uptake was observed in the brain and heart. (C) Comparison of the uptake of [ $^{18}\text{F}$ ]Glc1 (left) and [ $^{18}\text{F}$ ]FDG (right) in the brain. (D) Comparison of the uptake of [ $^{18}\text{F}$ ]Glc1 (left) and [ $^{18}\text{F}$ ]FDG (right) in the heart (orange arrow). The scale for [ $^{18}\text{F}$ ]Glc1 is 0–2 SUV and that for [ $^{18}\text{F}$ ]FDG is 0–5 SUV to enhance the difference.

## ■ ASSOCIATED CONTENT

### SI Supporting Information

The Supporting Information is available free of charge at <https://pubs.acs.org/doi/10.1021/acsomega.2c06551>.

Experimental synthetic and characterization details, NMR and mass spectral data, cytotoxicity, and radio-labeling (PDF)

## ■ AUTHOR INFORMATION

### Corresponding Authors

**Daniela Imperio** – Department of Pharmaceutical Sciences, University of Eastern Piedmont Amedeo Avogadro, 28100 Novara, Italy; [orcid.org/0000-0001-6810-1439](https://orcid.org/0000-0001-6810-1439); Email: [daniela.imperio@uniupo.it](mailto:daniela.imperio@uniupo.it)



Marcin Balcerzyk – Centro Nacional de Aceleradores, Universidad de Sevilla-CSIC-Junta de Andalucía, 41092 Sevilla, Spain; Departamento de Fisiología Médica y Biofísica, Universidad de Sevilla, 41003 Sevilla, Spain; Email: [mbalcerzyk@us.es](mailto:mbalcerzyk@us.es)

## Authors

Laura Confalonieri – Department of Pharmaceutical Sciences, University of Eastern Piedmont Amedeo Avogadro, 28100 Novara, Italy; [orcid.org/0000-0002-0236-9659](https://orcid.org/0000-0002-0236-9659)

Alvaro Erhard – Centro Nacional de Aceleradores, Universidad de Sevilla-CSIC-Junta de Andalucía, 41092 Sevilla, Spain

Silvia Fallarini – Department of Pharmaceutical Sciences, University of Eastern Piedmont Amedeo Avogadro, 28100 Novara, Italy

Federica Compostella – Department of Medical Biotechnology and Translational Medicine, University of Milan, 20133 Milano, Italy; [orcid.org/0000-0003-4721-0358](https://orcid.org/0000-0003-4721-0358)

Erika del Grosso – Department of Pharmaceutical Sciences, University of Eastern Piedmont Amedeo Avogadro, 28100 Novara, Italy

Luigi Panza – Department of Pharmaceutical Sciences, University of Eastern Piedmont Amedeo Avogadro, 28100 Novara, Italy; [orcid.org/0000-0002-0785-0409](https://orcid.org/0000-0002-0785-0409)

Complete contact information is available at:

<https://pubs.acs.org/10.1021/acsomega.2c06551>

## Author Contributions

The manuscript was written through the contributions of all authors

## Funding

The work was funded in part by Università del Piemonte Orientale A. Avogadro Progetto Ricerca Locale—(DSF) 2019, Fondazione CRT (Grant No. 236-2019 - id.406 for a fellowship to D.I.) and by Centro Nacional de Aceleradores, University of Seville, Spain. The authors thank Angel Luis Parrado-Gallego for participating in preclinical PET/CT experiments.

## Notes

The authors declare no competing financial interest.

## REFERENCES

- (1) Wang, S.; Zhang, Z.; Miao, L.; Li, Y. Boron Neutron Capture Therapy: Current Status and Challenges. *Front. Oncol.* **2022**, *12*, No. 788770.
- (2) Barth, R. F.; Mi, P.; Yang, W. Boron Delivery Agents for Neutron Capture Therapy of Cancer. *Cancer Commun.* **2018**, *38*, 35.
- (3) Jin, W. H.; Seldon, C.; Butkus, M.; Sauerwein, W.; Giap, H. B. A Review of Boron Neutron Capture Therapy: Its History and Current Challenges. *Int. J. Part. Ther.* **2022**, *9*, 71–82.
- (4) PMDA. List of Drugs Approved between April 2019 and March 2020. <https://www.pmda.go.jp/files/000235289.pdf> (accessed Nov 11, 2022).
- (5) Ali, F.; S Hosmane, N.; Zhu, Y. Boron Chemistry for Medical Applications. *Molecules* **2020**, *25*, 828.
- (6) Sauerwein, W. A. G.; Sancey, L.; Hey-Hawkins, E.; Kellert, M.; Panza, L.; Imperio, D.; Balcerzyk, M.; Rizzo, G.; Scalco, E.; Herrmann, K.; Mauri, P.; de Palma, A.; Wittig, A. Theranostics in Boron Neutron Capture Therapy. *Life* **2021**, *11*, 330.
- (7) Skwierawska, D.; López-Valverde, J. A.; Balcerzyk, M.; Leal, A. Clinical Viability of Boron Neutron Capture Therapy for Personalized Radiation Treatment. *Cancers* **2022**, *14*, 2865.
- (8) Imperio, D.; Muz, B.; Azab, A. K.; Fallarini, S.; Lombardi, G.; Panza, L. A Short and Convenient Synthesis of Closo-Dodecaborate Sugar Conjugates. *Eur. J. Org. Chem.* **2019**, *2019*, 7228–7232.
- (9) Imperio, D.; Panza, L. Sweet Boron: Boron-Containing Sugar Derivatives as Potential Agents for Boron Neutron Capture Therapy. *Symmetry* **2022**, *14*, 182.
- (10) Matović, J.; Järvinen, J.; Sokka, I. K.; Stockmann, P.; Kellert, M.; Imlimthan, S.; Sarparanta, M.; Johansson, M. P.; Hey-Hawkins, E.; Rautio, J.; Ekholm, F. S. Synthesis and *In Vitro* Evaluation of a Set of 6-Deoxy-6-Thio-Carboranyl <sc>d</sc>-Glucoconjugates Shed Light on the Substrate Specificity of the GLUT1 Transporter. *ACS Omega* **2022**, *7*, 30376–30388.
- (11) Imperio, D.; del Grosso, E.; Fallarini, S.; Lombardi, G.; Panza, L. Synthesis of Sugar–Boronic Acid Derivatives: A Class of Potential Agents for Boron Neutron Capture Therapy. *Org. Lett.* **2017**, *19*, 1678–1681.
- (12) Imperio, D.; del Grosso, E.; Fallarini, S.; Lombardi, G.; Panza, L. Anomeric Sugar Boronic Acid Analogues as Potential Agents for Boron Neutron Capture Therapy. *Beilstein J. Org. Chem.* **2019**, *15*, 1355–1359.
- (13) Muz, B.; Azab, A. K.; Confalonieri, L.; del Grosso, E.; Fallarini, S.; Imperio, D.; Panza, L. Synthesis, Equilibrium, and Biological Study of a C-7 Glucose Boronic Acid Derivative as a Potential Candidate for Boron Neutron Capture Therapy. *Bioorg. Med. Chem.* **2022**, *59*, No. 116659.
- (14) Itoh, T.; Tamura, K.; Ueda, H.; Tanaka, T.; Sato, K.; Kuroda, R.; Aoki, S. Design and Synthesis of Boron Containing Monosaccharides by the Hydroboration of D-Glucal for Use in Boron Neutron Capture Therapy (BNCT). *Bioorg. Med. Chem.* **2018**, *26*, 5922–5933.
- (15) Calvaresi, E. C.; Hergenrother, P. J. Glucose Conjugation for the Specific Targeting and Treatment of Cancer. *Chem. Sci.* **2013**, *4*, 2319.
- (16) Molander, G. A.; Sandrock, D. L. Potassium Trifluoroborate Salts as Convenient, Stable Reagents for Difficult Alkyl Transfers. *Curr. Opin. Drug Discovery Dev.* **2009**, *12*, 811–823.
- (17) Vedejs, E.; Chapman, R. W.; Fields, S. C.; Lin, S.; Schrimpf, M. R. Conversion of Arylboronic Acids into Potassium Aryltrifluoroborates: Convenient Precursors of Arylboron Difluoride Lewis Acids. *J. Org. Chem.* **1995**, *60*, 3020–3027.
- (18) Churches, Q. I.; Hooper, J. F.; Hutton, C. A. A General Method for Interconversion of Boronic Acid Protecting Groups: Trifluoroborates as Common Intermediates. *J. Org. Chem.* **2015**, *80*, 5428–5435.
- (19) Liu, Z.; Pourghasian, M.; Bénard, F.; Pan, J.; Lin, K.-S.; Perrin, D. M. Preclinical Evaluation of a High-Affinity <sup>18</sup>F-Trifluoroborate Octoate Derivative for Somatostatin Receptor Imaging. *J. Nucl. Med.* **2014**, *55*, 1499–1505.
- (20) Roxin, A.; Zhang, C.; Huh, S.; Lepage, M. L.; Zhang, Z.; Lin, K.-S.; Bénard, F.; Perrin, D. M. Preliminary Evaluation of <sup>18</sup>F-Labeled LLP2A-Trifluoroborate Conjugates as VLA-4 (A $\beta$ 1 Integrin) Specific Radiotracers for PET Imaging of Melanoma. *Nucl. Med. Biol.* **2018**, *61*, 11–20.
- (21) Balcerzyk, M.; De-Miguel, M.; Guerrero, C.; Fernandez, B. Quantification of Boron Compound Concentration for BNCT Using Positron Emission Tomography. *Cells* **2020**, *9*, 2084.
- (22) Liu, Z.; Chao, D.; Li, Y.; Ting, R.; Oh, J.; Perrin, D. M. From Minutes to Years: Predicting Organotrifluoroborate Solvolysis Rates. *Chem. - Eur. J.* **2015**, *21*, 3924–3928.
- (23) Li, J.; Shi, Y.; Zhang, Z.; Liu, H.; Lang, L.; Liu, T.; Chen, X.; Liu, Z. A Metabolically Stable Boron-Derived Tyrosine Serves as a Theranostic Agent for Positron Emission Tomography Guided Boron Neutron Capture Therapy. *Bioconjugate Chem.* **2019**, *30*, 2870–2878.
- (24) Banerjee, S. S.; Aher, N.; Patil, R.; Khandare, J. Poly(Ethylene Glycol)-Prodrug Conjugates: Concept, Design, and Applications. *J. Drug Delivery* **2012**, *2012*, 1–17.
- (25) Stoll, I.; Eberhard, J.; Brodbeck, R.; Eisfeld, W.; Mattay, J. A New Fluorescent Calix Crown Ether: Synthesis and Complex



Formation with Alkali Metal Ions. *Chem. - Eur. J.* **2008**, *14*, 1155–1163.

(26) Salman, A. A.; Heidelberg, T. In Situ Functionalized Fluorescent Nanoparticles for Efficient Receptor Coupling. *J. Nanopart. Res.* **2014**, *16*, 2399.

(27) Schofield, C. L.; Mukhopadhyay, B.; Hardy, S. M.; McDonnell, M. B.; Field, R. A.; Russell, D. A. Colorimetric Detection of Ricinus Communis Agglutinin 120 Using Optimally Presented Carbohydrate-Stabilised Gold Nanoparticles. *Analyst* **2008**, *133*, 626.

(28) Li, Z.; Chansaenpak, K.; Liu, S.; Wade, C. R.; Conti, P. S.; Gabbaï, F. P. Harvesting 18F-Fluoride Ions in Water via Direct 18F–19F Isotopic Exchange: Radiofluorination of Zwitterionic Aryltri-fluoroborates and in Vivo Stability Studies. *MedChemComm* **2012**, *3*, 1305.

(29) Schirmmacher, R.; Bradtmöller, G.; Schirmmacher, E.; Thews, O.; Tillmanns, J.; Siessmeier, T.; Buchholz, H. G.; Bartenstein, P.; Wängler, B.; Niemeyer, C. M.; Jurkschat, K. 18F-Labeling of Peptides by Means of an Organosilicon-Based Fluoride Acceptor. *Angew. Chem., Int. Ed.* **2006**, *45*, 6047–6050.

(30) Liu, Z.; Lin, K.-S.; Bénard, F.; Pourghasian, M.; Kiesewetter, D. O.; Perrin, D. M.; Chen, X. One-Step 18F Labeling of Biomolecules Using Organotrifluoroborates. *Nat. Protoc.* **2015**, *10*, 1423–1432.

## Recommended by ACS

### Green Surfactant Made from Cashew Phenol for Enhanced Oil Recovery

Junqi Wang, Kaili Liao, *et al.*

JANUARY 04, 2023  
ACS OMEGA

READ 

### Simple Multifunctional PTX@Ce6 Nanomedicine for Eradicating Tumor in the Combination of Photodynamic Therapy and Metronomic Chemotherapy

Mengxuan Li, Juan Li, *et al.*

DECEMBER 15, 2022  
ACS OMEGA

READ 

### Effect of Sandstone Wetting Reversal Induced by Low Temperature Plasma on the Oil Droplet Scouring under Flowing Water

Xiaoxiao Dou, Jianlin Liu, *et al.*

DECEMBER 09, 2022  
ACS OMEGA

READ 

### Exclusion of Anchor-Matched Peptide Nucleic Acid from Liquid-Ordered Domains by Hybridization with Complementary Flavin-Labeled DNA

Yoshimi Oka.

DECEMBER 16, 2022  
ACS OMEGA

READ 

Get More Suggestions >